Indian Geotechnical Journal, 37(3), 2007, 190-209

Analysis of Laterally Loaded Rigid Piles in Sands based on Kinematics and Non-linear Subgrade Response

V. Padmavathi*, E. Saibaba Reddy** and M. R. Madhav***

Introduction

Lateral forces affect structures such as transmission towers, tall buildings, abutments, port structures, offshore platforms, etc. The piles under these structures may experience lateral forces due to high wind forces, movement of vehicles, wave actions, earthquakes, etc. The lateral load capacity of pile foundations is thus critically important for the design of the superstructure. The ultimate lateral load carrying capacity of a single pile depends on the ultimate resistance offered by the surrounding soil, the pile flexibility, pile head and tip conditions.

Several methods are currently available for the prediction of the ultimate capacity of piles (Matlock and Reese 1960; Broms 1964; Reese et al. 1974; Poulos and Davis 1980; Meyerhof and Mathur 1981; Meyerhof and Sastry, 1985; Prakash and Kumar 1996; Prasad and Chari 1999; Patra and Pise 2001; Shen and Teh 2004; Zhang et al. 2005). All these studies consider only the fully plastic state of the soil with no consideration of the kinematics of pile movement. Therefore, the predictions based on most of these methods result not only in different ultimate capacities, but also differ from the actual values, because the ultimate capacity of a laterally loaded pile is dependent on the actual kinematics and the non-linear response of the soil.

In this paper a new approach, that considers the kinematics of pile displacements and non-linear subgrade reaction is presented for the prediction of the ultimate lateral load capacity of a single rigid free-head pile in cohesionless soil. The ultimate capacities and variations of lateral soil pressures with depth based on the proposed approach are compared with other theoretical approaches and experimental results from small scale and in-situ tests available in literature.

* Assistant Professor, Dept. of Civil Engineering, J. N. T. U. College of Engineering, Hyderabad - 500 072, India. Email: padmavathiv_2000@yahoo.com

** Professor, Dept. of Civil Engineering, J. N. T. U. College of Engineering, Hyderabad - 500 072, India. Email: reddysaibaba@rediffmail.com

*** Emeritus Professor, Dept. of Civil Engineering, J. N. T. U. College of Engineering, Hyderabad - 500 072, India. Email: madhav@iitk.ac.in

Ultimate Lateral Soil Pressure

Several methods are available for determining the ultimate lateral capacity of rigid piles in cohesionless soils based on the ultimate soil pressure distribution along the pile length. Some of these methods are:

Hansen (1961) predicted the ultimate lateral capacity of the pile based on ultimate lateral soil pressure, p_u, of cohesionless soil as

$$p_u = K_q \gamma z B \qquad (1)$$

where K_q = the earth pressure coefficient - a function of ϕ', the angle of shearing resistance of the soil, γ = effective unit weight of the soil, z = depth from the ground surface and B = diameter or width of the pile.

Broms (1964) considered the three - dimensional effect and proposed that the ultimate lateral soil pressure in cohesionless soils can be three times the passive pressure as

$$p_u = 3K_p \gamma z B \qquad (2)$$

where $K_p = \tan^2(45+\phi'/2)$ – the Rankine passive earth pressure coefficient.

Predictions based on Broms approach [Equation (2)] overestimate the ultimate capacities by about 30% when compared with field test results (Poulos and Davis 1980). Reese et al. (1974) suggested a more complex variation of ultimate lateral pressure of soil with depth, taking due account of the wedge type failure near the ground surface. The ultimate lateral pressure of the soil is initially proportional to K_p at shallow depths, but becomes proportional to K_p^3 at greater depths.

A variation intermediate between the above two variations of ultimate lateral soil pressure with depth was given by Fleming et al. (1992) as

$$p_u = K_p^2 \gamma z B \qquad (3)$$

For most natural sands K_p is greater than 3. Therefore, Equation 3 gives a better fit to results of load tests but overestimates the values of ultimate lateral capacity by about 6%, which is considerably less compared to Broms predictions (Barton 1982).

All the above approaches are based on the assumption that the ultimate soil pressure is mobilized on the pile surface projected on to a vertical plane and as an extension of the concept of lateral pressures on retaining walls.

Prasad and Chari (1999) suggest the ultimate lateral pressure of the soil on the pile to be

$$p_u = s\, f(\phi) \gamma z \qquad (4)$$

where f (ϕ) – a function of earth pressure coefficient K_p, s – a shape factor which depends on ϕ. The value of sK_p is given as $10^{(1.3\tan\phi + 0.3)}$.

Zhang et al. (2005) are probably the first to consider the ultimate lateral soil pressure exerted by the soil against the pile as the sum of the normal soil pressure on the projected area and the side-shear resistance. The ultimate lateral soil pressure, p_u, is given as

$$p_u = (\eta\, p_{max} + \xi\, \tau_{max})B \tag{5}$$

where η = a shape factor to account for the non-uniform distribution of soil pressure normal to the pile, $p_{max} = K_p^2\gamma z$ - maximum lateral soil pressure which is the same as that given by Fleming et al. (1992), ξ = shape factor to account for non-uniform distribution of side shear or drag and $\tau_{max} = K\gamma z \tan\delta$ - maximum side shear resistance, K = lateral earth pressure coefficient and δ = pile-soil interface friction angle. η and ξ values (Briaud and Smith 1983) are given in Table 1. Values of K and δ reported in the literature (Poulos and Davis 1980; NAVFAC 1982; Kulhawy et al. 1983; Kulhawy 1984,1991; Tomlinson 1986; API 1991; Randolph et al. 1994; Wong and Teh 1995) are summarized in Tables 2 and 3.

TABLE 1: Values of η and ξ (after Briaud and Smith 1983)

Pile shape	H	ξ
Circular	0.8	1.0
Square	1.0	2.0

TABLE 2: Values of K (Kulhawy et al. 1983 and Kulhawy 1991)

Pile type and method of construction	K
Pile-jetted	(0.5 - 0.7) K_0
Pile-small displacement, driven	(0.7 - 1.2) K_0
Pile-large displacement, driven	(1.0 - 2.0) K_0
Drilled shaft-build using dry method with minimal sidewall disturbance and prompt concreting	(0.9 - 1.0) K_0
Drilled shaft-slurry construction with good workmanship	(0.9 - 1.0) K_0
Drilled shaft-slurry construction with poor workmanship	(0.6 - 0.7) K_0
Drilled shaft-casing method below water table	(0.7 - 0.9) K_0

where K_0 = coefficient of lateral earth pressure at rest.

TABLE 3: Recommended Values of δ by Kulhawy et al. (1983) and Kulhawy (1991)

Pile type	δ
Rough concrete	1.0 ϕ'
Smooth concrete (i.e. precast pile)	(0.8-1.0) ϕ'
Rough steel (i.e. step-taper pile)	(0.7-0.9) ϕ'
Smooth steel (i.e. pipe pile or H pile)	(0.5-0.7) ϕ'
Wood (i.e. timber pile)	(0.8-0.9) ϕ'
Drilled shaft built using dry method or with temporary casing and good construction techniques	1.0ϕ'
Drilled shaft built with slurry method (higher values correspond to more careful construction methods)	(0.8-1.0) ϕ'

Lateral Soil Pressure Distributions

The lateral soil pressure distribution along the pile length at ultimate lateral load according to Broms (1964) is shown in Figure 1(a). For simplicity, Broms (1964) considers soil pressure to increase linearly from zero at the ground surface to a maximum at the toe of the pile. The soil pressures acting in the opposite direction on the rear side of the pile below the point of rotation and those added on the front side for simplifying the distribution are replaced by a point load at the tip of the pile on the rear side.

According to Prasad and Chari (1999), based on test results (Figure 1(b)), the soil pressure is zero at the ground surface and increases with depth upto 0.6 times depth of point of rotation, z_0. At a depth 0.6 z_0 the soil pressure is $10^{(1.3\tan\phi + 0.3)}\gamma\, 0.6z_0$. The pressure decreases linearly until it reduces to zero at the point of rotation, i.e. at a depth of z_0. Below z_0, the net soil pressure that acts on the rear side of the pile increases linearly from zero at depth z_0, to a maximum value of 1.7 times the soil pressure at 0.6 z_0 depth at the tip of the pile.

Zhang et al. (2005) proposed both normal soil pressure as well as side-shear distributions to vary with depth as depicted in Figures 1(c) & (d). The normal soil pressure and side-shear distributions are the same as those of Prasad and Chari (1999) but the values of normal soil pressure and side shear at $0.6z_0$ depth are $\eta BK_p^2\gamma.0.6z_0$ and $\xi BK\gamma(0.6z_0)\tan\delta$ respectively. At the toe of the pile, pressures are 1.7 times the pressures at depth $0.6z_0$ but in the opposite direction.

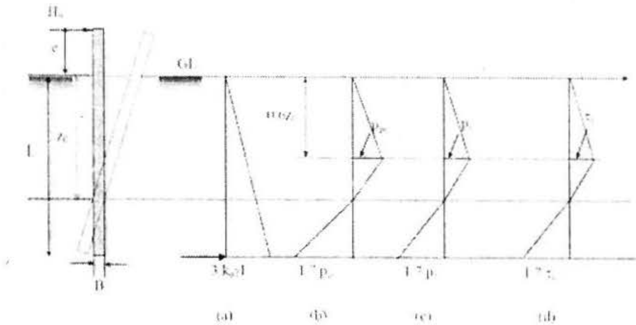

Fig. 1 Assumed Soil Pressure Distribution under Ultimate Lateral Load by Different Methods (a) Broms (1964) (b) Prasad & Chari (1999) (c) & (d) Zhang et al. (2005) Normal and Side Shear Resistances

Problem Statement

A short rigid pile of embedded length, L, and diameter, d, is acted upon by a lateral force, H, at an eccentricity, e, creating a moment, M (= e × H), at the ground level (Figure 2). The pile is unrestrained and rotates through an angle θ, about a point at depth, z_0, from the ground surface. The displacements thus vary linearly with depth. The response of the soil on to the pile is represented by non-linear Winkler type response with modulus of subgrade reaction, k_s, and ultimate lateral soil pressure, q_{max}. The lateral stress, q, is related (Figure 3) to the lateral displacement ρ, as

$$q = \frac{k_s \rho_z}{1 + \frac{k_s \rho_z}{q_{\max}}} \tag{6}$$

where ρ_z = $(z_0 - z)\tan\theta$ is the displacement of the pile at depth z, from ground surface. Both k_s and q_{max} are assumed to increase linearly with depth as

$k_s = \alpha_k.z/L$, and (7)

$q_{max} = \alpha_q.z/L$ (8)

where α_k and α_q are the rates of increase respectively of the modulus of subgrade reaction and the maximum lateral soil pressure with depth.

The depth of point of rotation, z_0, and the angle of the rotation θ, of the pile are the two unknowns. For equilibrium, the applied lateral force H, is equated to the total response from the soil as

$H = Q^+ + Q^-$ (9)

where Q^+ and Q^- are the total soil response forces above and below the point of rotation and equal $\int_0^{z_0} q_t d.dz$ and $\int_{z_0}^{L} q_b d.dz$ respectively.

where q_t and q_b are the lateral stresses above and below the point of rotation respectively. Equation 9 becomes

$$H = \int_0^{z_0} \frac{k_s \rho_z d}{1 + \frac{k_s \rho_z}{q_{max}}} dz - \int_{z_0}^{L} \frac{k_s \overline{\rho_z} d}{1 + \frac{k_s \overline{\rho_z}}{q_{max}}} dz \quad (10)$$

where $\rho_z = (z_0 - z)\tan\theta$ and $\overline{\rho_z} = (z - z_0)\tan\theta$ are displacements above and below the point of rotation at depth z. Substituting Equations (7) and (8) in Equation (10) and rearranging the terms Equation (10) gets transformed in to normalized form as

$$H^* = \frac{H}{\alpha_k d L^2} = \int_0^{\overline{z_0}} \frac{\overline{z}(\overline{z_0} - \overline{z})\tan\theta}{1 + \mu(\overline{z_0} - \overline{z})\tan\theta} d\overline{z} - \int_{\overline{z_0}}^{1} \frac{\overline{z}(\overline{z} - \overline{z_0})\tan\theta}{1 + \mu(\overline{z} - \overline{z_0})\tan\theta} d\overline{z} \quad (11)$$

where normalized depth, $\overline{z}$ = z/L, normalized depth of point of rotation, $\overline{z_0} = z_0 / L$, and normalized load, $H^* = \frac{H}{\alpha_k d L^2}$. The parameter, μ along with Equations (7) and (8) can be defined as

$$\mu = \frac{k_s L}{q_{max}} = \frac{\alpha_k L}{\alpha_q} \quad (12)$$

Taking moments about the point of application of the load, the normalized form of the relation becomes

$$M^* = \frac{M}{\alpha_k d L^3} = \frac{He}{\alpha_k d L^3}$$
$$= \int_0^{\overline{z_0}} \frac{\overline{z}^2 (\overline{z_0} - \overline{z})\tan\theta}{1 + \mu(\overline{z_0} - \overline{z})\tan\theta} d\overline{z} - \int_{\overline{z_0}}^{1} \frac{\overline{z}^2 (\overline{z} - \overline{z_0})\tan\theta}{1 + \mu(\overline{z} - \overline{z_0})\tan\theta} d\overline{z} \quad (13)$$

Ideally, the depth of rotation, z_0, and the rotation, θ, are to be estimated for given lateral force, H, and moment, M. However, it would be an iterative process and very tedious. Alternately, for given values of μ and θ, $\overline{z_0}$ and H^* can be obtained by solving Equations (11) and (13). Knowing $\overline{z_0}$ and θ, the normalized deflection at ground level, $\rho^* = \overline{z_0} \tan\theta$, is calculated corresponding to the normalized applied load, H^*.

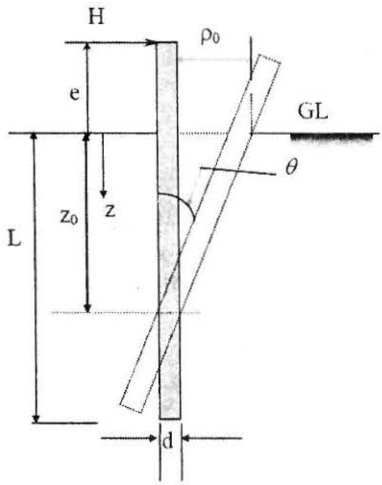

Fig. 2 Definition Sketch

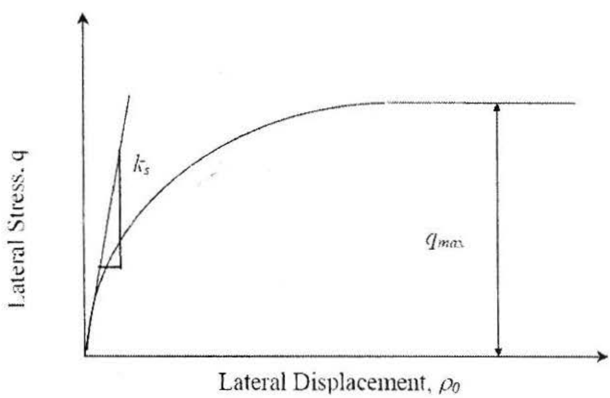

Fig. 3 Non-Linear Hyperbolic Response of the Soil

The Parameters

The modulus of subgrade reaction for granular materials is known to increase linearly with depth (Reese and Matlock 1956) as

$$k_s = n_h z / d = \alpha_k z / L \tag{14}$$

where n_h is coefficient of modulus of subgrade reaction. The values of n_h for different soils are given in Table 4 (after Terzaghi 1955 from Poulos and Davis 1980). The ultimate lateral pressure of the soil, $q_{max} = p_u/B$ can be obtained from any of the Equations (1) through (5). μ is then estimated from the values of n_h, q_{max} and L using Equation (12).

Results

The variation of H^* with ρ^* based on the proposed model is presented in Figure 4 for μ values ranging from 0 to 2000 and for no moment at ground level. The normalized lateral load, H^* increases as expected with normalized displacement at GL. The curve is linear for $\mu = 0$, i.e. very large (infinite) value of ultimate lateral pressure of the soil, q_{max}. With increasing values of μ, the normalized ultimate lateral pressure of the pile decreases but is attained at very large displacements. Very low ultimate capacities of the pile are attained at relatively smaller lateral displacements only for very large value of μ, i.e. smaller ultimate soil resistances. For values of μ in the range $200 > \mu > 0$, precise ultimate lateral resistances of the pile cannot be discerned from the curves in Figure 4.

TABLE 4: Values of n_h (MN/m^3) for Sand (after Terzaghi 1955)

Relative density	Loose	Medium	Dense
n_h dry or moist sand	2.1	6.3	16.8
n_h submerged sand	0.9	4.2	10.2

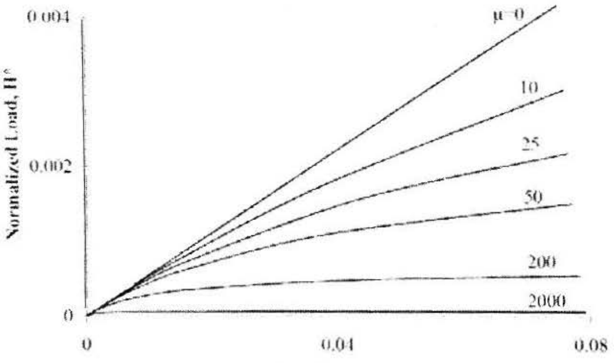

Fig. 4 Normalized Load vs. Displacement at GL for Zero Moment

Estimation of Ultimate Lateral Capacity of the Pile

Kondner's (1960) hyperbolic plot is utilized for the estimation of the ultimate lateral capacities of the pile. The ratio ρ^*/H^* was plotted against ρ^*, to obtain a straight line. The reciprocal of the slope of the straight line is the normalized ultimate lateral load, H_u^*. The ultimate lateral capacity of the pile is then calculated from the expression

$$H_u = H_u^* \alpha_k d L^2 \tag{15}$$

Comparisons

Broms Method

The maximum lateral soil pressure against the pile, q_{max}, can vary from 3 to 9 times the Rankine's passive earth pressure (Broms 1964). μ values have been estimated for various n_h, q_{max} and L values. For different μ and θ, values of normalized displacements ρ^*, of a pile at ground level were evaluated corresponding to the normalized forces, H^*, and with zero eccentricity (e = 0) and shown in Figure 4. For each μ value the corresponding ultimate lateral load on to the pile are estimated using Equation (15). Substituting for α_k as $\mu\ \alpha_q / L$, and α_q as n $K_p\gamma L$ and dividing by $K_p\gamma\ d^3$, Equation (15) can be written as

$$\frac{H_u}{K_p \gamma d^3} = nH_u^* \mu (L/d)^2 \tag{16}$$

where n is a parameter which varies from 3 to 9

For different values of L/d, values of $H_u/(K_p\gamma\, d^3)$ were obtained for known soil properties and pile dimensions. $H_u/(K_p\gamma\, d^3)$ values from Broms (1964) and proposed methods for $q_{max} = 3K_p\gamma z$ and different μ values are presented in Figure 5. Ultimate lateral load capacity of the piles is over-predicted by Broms (1964) approach by about 30 to 60% because of the consideration of full mobilization of soil pressure close to the point of rotation (Figure 1(a)) even though the displacement there is zero. It is also difficult to assign an exact value to 'n' for the determination of q_{max} because according to Broms theory, it can vary from 3 to 9.

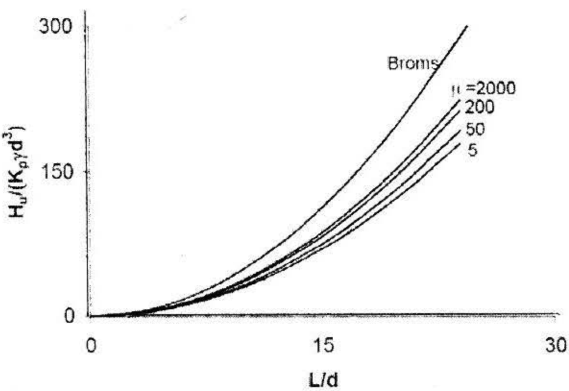

Fig. 5 Comparison of Predicted Ultimate Lateral Loads with Broms (1964) for $q_{max} = 3k_p\gamma z$

Prasad and Chari (1999) Method

Prasad and Chari (1999) proposed Equation (4) for the variation of lateral soil pressure along the length of the pile, as shown in Figure1(b). In addition, they propose a factor 0.8 to account for non-uniform distribution of lateral pressure on the pile width. Hence, for different values of μ and L/d and with q_{max} = $0.8\,sK_p\gamma\, z$, values of $H_u/(sK_p\gamma\, d^3)$ were obtained (Figure 6). Results from Prasad and Chari (1999) agree closely with those from the method for low values of μ (<5). As value of μ increases the ultimate capacities predicted by the proposed method are higher than those from Prasad and Chari (1999). These differences increase with increasing values of L/d. The differences in the ultimate loads from the two methods range between 1 to 25%, possibly be due to the assumption that the frontal soil pressure is maximum at a distance of 0.6 times the depth of the point of rotation, z_0, from ground level in the case of Prasad and Chari (1999) while no such assumption is required to be made in the present method.

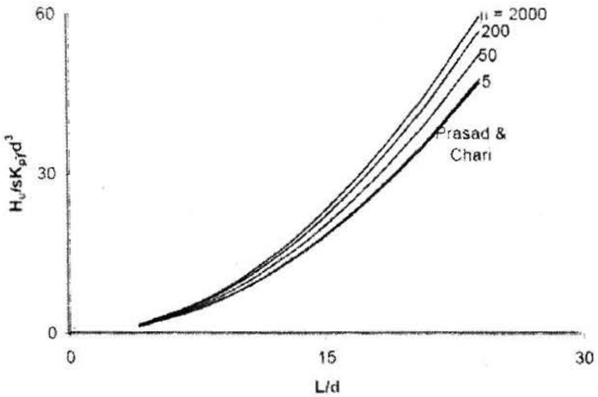

Fig. 6 Comparison of Predicted Ultimate Lateral Loads with Prasad & Chari (1999) for $q_{max} = 0.8sK_p\gamma z$ and e = 0

Zhang et al. (2005) Method

Zhang et al. (2005) proposed Equation (5) which considers the variations of lateral pressures due to normal soil pressure and side-shear along the length of the pile as shown in Figures 1(c) & (d). For typical soil properties, of $\phi = 30°$, $\delta = \phi$, $K = K_0$ the ratio of side shear and normal pressure (=$\xi\, K\gamma z \tan\delta/\eta\, K_p^2\gamma z$) is only 0.04. Hence, the contribution of side shear can be neglected. Values of $H_u/(K_p^2\gamma\, d^3)$ were obtained for different values of μ, L/d and q_{max}= 0.8 $K_p^2\gamma\, z$ (Figure 7). The trends in the results are almost the same as those of Prasad and Chari (1999). Based on the above results, the contribution of side shear resistance is considered to be negligible and hence not included further in this study. The ultimate lateral soil pressure, q_{max}, the soil can mobilize is limited to 0.8 $K_p^2\gamma\, z$.

Comparison of Predicted Ultimate Capacities with Measured Test Data

While a large body of test results giving only the ultimate capacities of piles tested is available, only a few test results are available which present the complete load-displacement plots for the piles tested. The proposed method based on kinematics and non-linear load displacement response of the soil requires the latter. The slope of the experimental load-displacement curve is utilized to estimate the value of n_h, as $n_h = 18H(1+1.33*e/L)/(\rho L^2)$. The maximum lateral pressure of the soil, q_{max}, is taken as $0.8K_p^2\gamma z$ (Zhang et al. 2005). The parameter, μ, is evaluated as given in Equation (12) with the above values of n_h and q_{max}.

The variation of normalized load with normalized displacement at ground level is predicted for the estimated values of μ and for different values of $\tan\theta$ based on which the ultimate lateral capacity of the piles are obtained. The estimated ultimate lateral loads of the piles are compared with the experimental values (Table 5). The agreement with the experimental data is good and the error being less than 30% for almost all the cases and the methods considered.

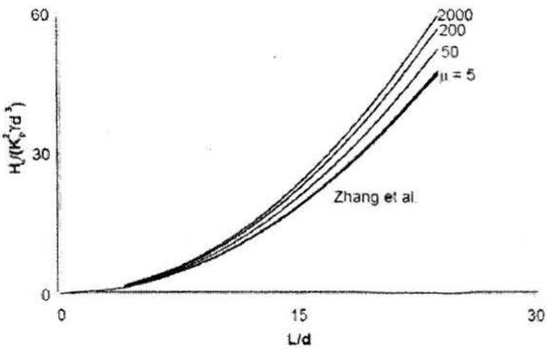

Fig. 7 Comparison of Predicted Ultimate Lateral Loads with Zhang et al. (2005) for $q_{max} = \eta k_p^2\gamma z$ and e = 0

TABLE 5: Comparison of Predicted and Observed Ultimate Capacities
(Obs. = Observed; Pred. = Predicted)

Sl. No	Pile dimensions		Soil properties		e (mm)	Obs. H_u (kN)	Pred. H_u (kN)	References
	L (mm)	B (mm)	γ (kN/m^3)	ϕ' (°)				
1	444.5	101.6	15.7	31	317.5	0.15	0.164	Adams and Radhakrishna (1973)
2	444.5	101.6	17.6	45	317.5	0.54	0.645	
3	444.5	76.2	17.6	45	317.5	0.41	0.483	
4	444.5	50.8	17.6	45	317.5	0.34	0.321	
5	200.0	12.5	15.2	50	0	0.04	0.041	Meyerhof et al. (1981)
6	200.0	12.5	14.0	35	0	0.011	0.009	
7	612.0	102.0	16.5	35	150.0	0.62	0.629	Prasad and Chari (1999)
8	612.0	102.0	17.3	41	150.0	1.04	1.102	
9	612.0	102.0	18.3	45.5	150.0	1.79	1.8	
10	991.0	75.0	15	46	75.0	2.05	3.84	Chari and Meyerhof (1983)
11	1500	101.6	17.66	35	0	8.8	5.68	Nabil F. Ismael (1989)

Ultimate lateral loads of the piles based on Broms (1964), Prasad and Chari (1999), Zhang et al. (2005) theories and the proposed method are compared in Table 6. Broms (1964), Prasad and Chari (1999) values are on the higher side compared to the experimental data whereas Zhang et al. (2005) and the proposed method give values close to the experimental ones with minimum error. The measured and predicted (from all the above approaches) H_u values reported in Tables 5 and 6 are collated in Figure 8. The values lie close to the 45° line indicating a good fit between the predictions and the observed values.

TABLE 6: Comparison of Ultimate Lateral Loads

References	Details of testing	Observed Load (kN)	Predicted load (kN) by different methods			
			Broms (1964)	Prasad and Chari (1999)	Zhang et al. (2005)	Proposed
Adams and Radhakrishna (1973)	L=444.5 mm B=101.6 mm e=317.5 mm γ= 15.7 kN/m^3 ϕ' = 31°	0.152	0.29	0.151	0.13	0.164
	L=444.5 mm B=101.6 mm e=317.5 mm γ= 17.6 kN/m^3 ϕ' = 45°	0.54	0.601	0.558	0.48	0.645
	L=444.5 mm B=76.2 mm e=317.5 mm γ= 17.6 kN/m^3 ϕ' = 45°	0.41	0.45	0.419	0.36	0.483
	L=444.5 mm B=50.8 mm e=317.5 mm γ= 17.6 kN/m^3 ϕ' = 45°	0.34	0.3	0.28	0.24	0.321
Meyerhof et al. (1981)	L=200.0 mm B=12.5 mm e=0 mm γ= 15.2kN/m^3 ϕ' = 50°	0.04	0.029	0.044	0.036	0.041
	L=200.0 mm B=12.5 mm e=0 mm γ= 14kN/m^3 ϕ' = 35°	0.011	0.013	0.01	0.008	0.009
Prasad and Chari (1999)	L=612.0 mm B=102.0 mm e=150.0 mm γ= 16.5 kN/m^3 ϕ' = 35°	0.62	0.934	0.62	0.53	0.629
	L=612.0 mm B=102.0 mm e=150.0 mm γ= 17.3 kN/m^3 ϕ' = 41°	1.04	1.277	1.075	0.94	1.102
	L=612.0 mm B=102.0 mm e=150.0 mm γ= 18.3 kN/m^3 ϕ' = 45.5°	1.79	1.677	1.77	1.52	1.8
Chari and Meyerhof (1983)	L=991 mm B=75 mm e=75 mm γ= 15 kN/m^3 ϕ' = 48°	2.05	3.15	3.61	3.09	3.84
Nabil F. Ismael (1989)	L=1500 mm B=101.6mm e=0 mm γ=17.66kN/m^3 ϕ' = 35°	8.8	7.4	5.36	4.79	5.68

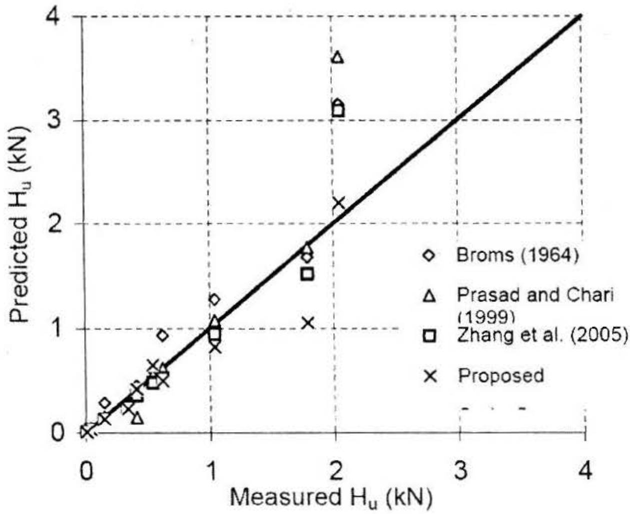

Fig. 8 Comparison of Measured and Predicted Hu Values

Comparison of Variations of Lateral Soil Resistance with Depth

Adams and Radhakrishna (1973), Chari and Meyerhof (1983), Prasad and Chari (1999) measured actual lateral soil pressures along the pile length using pressure transducers (Table 7). For each case listed in Table 7, variations of measured lateral pressure of the soil along the length of the pile are compared with the estimated or predicted (by Prasad and Chari 1999; Zhang et al. 2005; and the proposed approaches) values for the same lateral displacement of the ground point.

TABLE 7: Details of Test Piles for Comparison of Soil Pressures along the Length of the Pile

Case	Pile dimensions		Soil properties		Eccentricity of loading, e (mm)	References
	L (mm)	B (mm)	γ (kN/m^3)	ϕ' (°)		
1	444.5	101.6	15.7	31	317.5	Adams and Radhakrishna (1973)
2	444.5	101.6	17.6	45	317.5	
3	991.0	75.0	15	46	75.0	Chari and Meyerhof (1983)
4	612.0	102.0	16.5	35	150.0	Prasad and Chari (1999)
5	612.0	102.0	17.3	41	150.0	
6	612.0	102.0	18.3	45.5	150.0	

Adams and Radhakrishna (1973) tested model rigid piles of 444.5 mm length, 101.6 mm diameter and 317.5 mm load eccentricity in loose and dense sand conditions for ϕ = 31° and 45° respectively. Figure 9 compares the measured and predicted lateral soil pressure distributions for tests in loose sand. Prasad and Chari (1999) overestimate the lateral soil pressure distribution profile while the profile predicted by Zhang et al. (2005) is close to the experimental curve. However, both the approaches predict linear variation of lateral soil pressure along the pile while the actual variation is non-linear. The lateral soil pressure variation predicted by the proposed method is non-linear and close to the experimental curve. Figure 10 compares the results for tests in dense sands for the same model piles. The profile by the present approach is closer to the experimental points compared to the profiles by Prasad and Chari (1999) and Zhang et al. (2005).

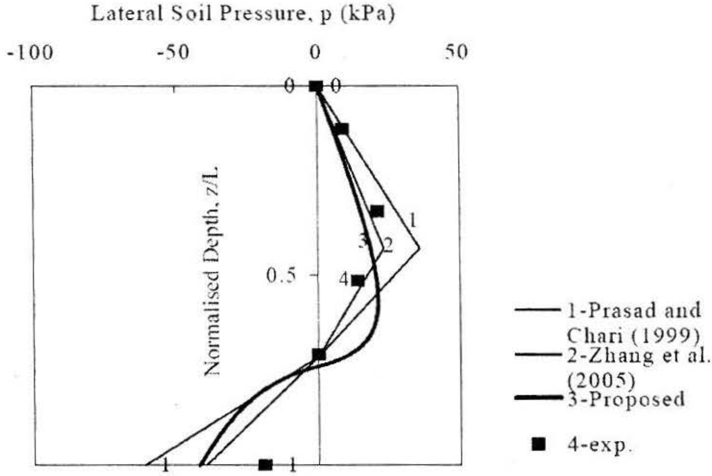

Fig. 9 Lateral Soil Pressure with Respect to Depth along Pile Length – Case 1

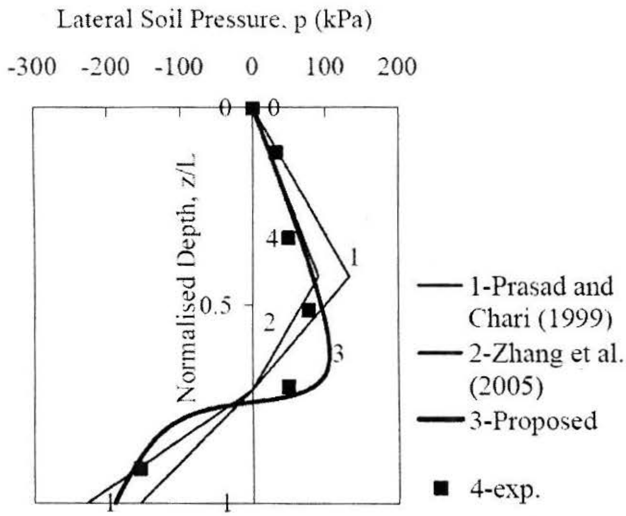

Fig. 10 Lateral Soil Pressure with Respect to Depth along Pile Length – Case 2

Chari and Meyerhof (1983) conducted tests on smooth steel model pile, 75 mm in diameter and buried 991 mm into sand and with an eccentricity of 75 mm. The angle of internal friction of the sand was 46°. Figure 11 compares the lateral pressure distributions with depth. While the approach by Prasad and Chari (1999) yields higher values of lateral soil pressure, Zhang et al. (2005)

and the proposed approaches predict variations that are close to each other and the measured values.

Prasad and Chari (1999) conducted tests on smooth steel model pile, of diameter 102.0 mm, embedment depth of 612.0 mm and 150 mm load eccentricity. Tests were conducted in sands having $\phi = 35°, 41°$ and $45.5°$. The comparisons of variations of lateral pressures with depth are shown in Figure 12, for $\phi = 35°$. The lateral soil pressure profile predicted by Prasad and Chari's method (1999) is closer to the experimental one while those by Zhang et al. (2005) and present methods are on the lower side but not considerably. Similar trends are observed for $\phi = 41°$ and $45.5°$ (Figures 13 and 14).

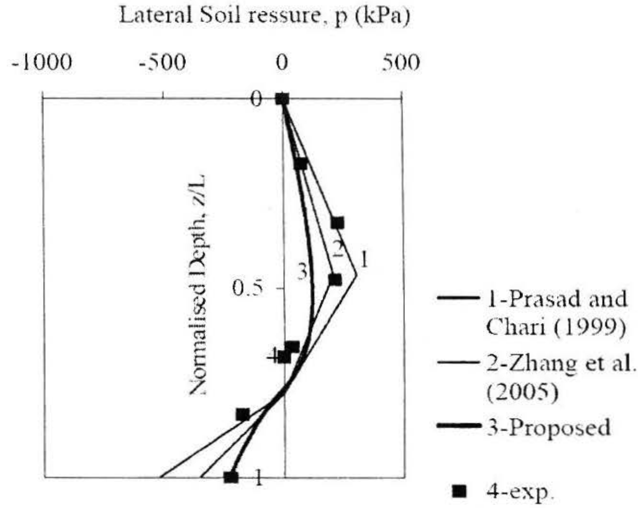

Fig. 11 Lateral Soil Pressure with Respect to Depth along Pile Length – Case 3

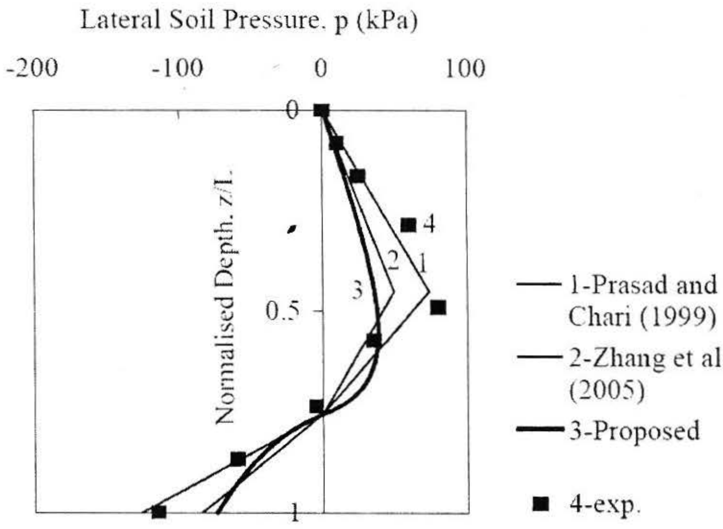

Fig. 12 Lateral Soil Pressure with Respect to Depth along Pile Length – Case 4

Conclusions

The ultimate lateral capacity of a rigid pile in cohesionless soil depends on the magnitude and distribution of lateral soil pressure along its length. An approach considering the kinematics and obviating the need to make simplifying assumptions for the variation of lateral soil pressure and considering non-linear response of the soil is presented for the estimation of load – displacement response and the ultimate lateral capacity of the pile. The ultimate load the pile can carry thus depends not only on the ultimate or maximum lateral soil pressure but also on the variation of the subgrade modulus with depth. The ultimate lateral capacity of the pile and the variation of lateral soil pressure with depth predicted by the proposed approach compare well with those predicted by other available ones and with the measured values. The maximum difference is well within 30%.

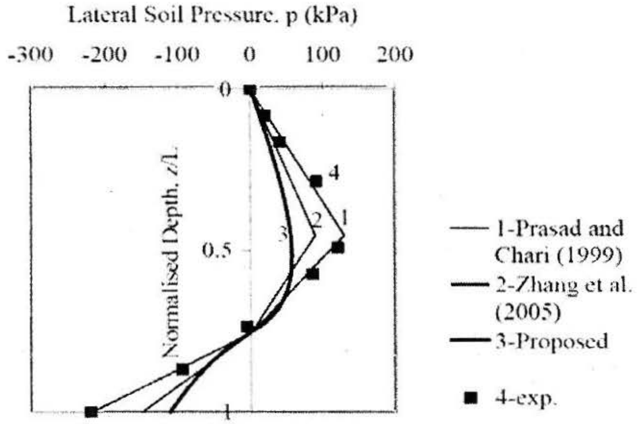

Fig. 13 Lateral Soil Pressure with Respect to Depth along Pile Length – Case 5

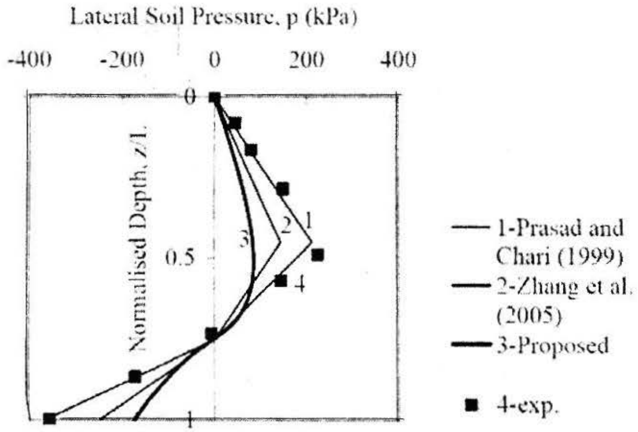

Fig. 14 Lateral Soil Pressure with Respect to Depth along Pile Length – Case 6

The normalized ultimate lateral capacities, $H_u/K_p^2\gamma d^3$, of the pile with $p_{max} = 0.8\ K_p^2\gamma z$, are given for ready reference in Table 8 and Figures 15 and 16 for different values of μ, e, and L/d.

TABLE 8: Values of Normalized Ultimate Capacity $H_u / (K_p^2 \gamma d^3)$

		L/d					
μ	e	4	8	12	16	20	24
5	0	1.224	4.894	11.012	19.577	30.589	44.048
	0.2	1.008	4.031	9.070	16.125	25.195	36.281
	0.4	0.869	3.476	7.822	13.906	21.728	31.288
	0.6	0.731	2.924	6.578	11.694	18.272	26.312
	0.8	0.662	2.649	5.959	10.594	16.554	23.837
	1	0.564	2.256	5.077	9.026	14.102	20.307
	2	0.372	1.487	3.345	5.947	9.293	13.382
	4	0.210	0.842	1.894	3.368	5.262	7.578
10	0	1.366	5.463	12.291	21.850	34.141	49.163
	0.2	1.095	4.378	9.851	17.512	27.363	39.403
	0.4	0.900	3.601	8.102	14.404	22.506	32.408
	0.6	0.771	3.082	6.935	12.329	19.264	27.740
	0.8	0.665	2.661	5.987	10.643	16.630	23.948
	1	0.591	2.365	5.322	9.462	14.784	21.289
	2	0.368	1.474	3.315	5.894	9.210	13.262
	4	0.215	0.860	1.935	3.441	5.376	7.741
25	0	1.416	5.665	12.747	22.661	35.408	50.988
	0.2	1.131	4.524	10.178	18.094	28.272	40.712
	0.4	0.946	3.785	8.516	15.140	23.656	34.065
	0.6	0.797	3.188	7.174	12.754	19.928	28.696
	0.8	0.703	2.813	6.330	11.254	17.584	25.321
	1	0.618	2.473	5.564	9.892	15.456	22.257
	2	0.394	1.576	3.545	6.303	9.848	14.181
	4	0.227	0.906	2.039	3.625	5.664	8.156
50	0	1.480	5.919	13.317	23.675	36.992	53.268
	0.2	1.175	4.700	10.575	18.801	29.376	42.301
	0.4	0.975	3.901	8.778	15.606	24.384	35.113
	0.6	0.832	3.328	7.488	13.312	20.800	29.952
	0.8	0.724	2.898	6.520	11.592	18.112	26.081
	1	0.642	2.568	5.777	10.271	16.048	23.109
	2	0.408	1.631	3.669	6.523	10.192	14.676
	4	0.236	0.942	2.120	3.768	5.888	8.479
100	0	1.531	6.124	13.778	24.494	38.272	55.112
	0.2	1.220	4.879	10.979	19.517	30.496	43.914
	0.4	1.011	4.045	9.101	16.179	25.280	36.403
	0.6	0.863	3.451	7.764	13.804	21.568	31.058
	0.8	0.753	3.011	6.774	12.042	18.816	27.095
	1	0.667	2.668	6.002	10.670	16.672	24.008
	2	0.424	1.695	3.813	6.779	10.592	15.252
	4	0.244	0.978	2.200	3.912	6.112	8.801
200	0	1.580	6.318	14.216	25.272	39.488	56.863
	0.2	1.260	5.038	11.336	20.152	31.488	45.343
	0.4	1.044	4.178	9.400	16.712	26.112	37.601

(Continuation in next page)

	0.6	0.891	3.564	8.018	14.254	22.272	32.072
	0.8	0.776	3.103	6.981	12.411	19.392	27.924
	1	0.686	2.744	6.175	10.977	17.152	24.699
	2	0.438	1.751	3.940	7.004	10.944	15.759
	4	0.252	1.008	2.267	4.030	6.298	9.069
500	0	1.626	6.502	14.630	26.010	40.640	58.522
	0.2	1.293	5.171	11.635	20.685	32.320	46.541
	0.4	1.075	4.301	9.677	17.203	26.880	38.707
	0.6	0.915	3.661	8.237	14.643	22.880	32.947
	0.8	0.800	3.200	7.200	12.800	20.000	28.800
	1	0.704	2.816	6.336	11.264	17.600	25.344
	2	0.449	1.795	4.038	7.178	11.216	16.151
	4	0.259	1.037	2.333	4.147	6.480	9.331
1000	0	1.638	6.554	14.746	26.214	40.960	58.982
	0.2	1.306	5.222	11.750	20.890	32.640	47.002
	0.4	1.087	4.347	9.780	17.388	27.168	39.122
	0.6	0.927	3.707	8.340	14.828	23.168	33.362
	0.8	0.808	3.231	7.269	12.923	20.192	29.076
	1	0.716	2.862	6.440	11.448	17.888	25.759
	2	0.454	1.818	4.090	7.270	11.360	16.358
	4	0.262	1.050	2.362	4.198	6.560	9.446
5000	0	1.658	6.630	14.918	26.522	41.440	59.674
	0.2	1.325	5.299	11.923	21.197	33.120	47.693
	0.4	1.094	4.378	9.850	17.510	27.360	39.398
	0.6	0.934	3.738	8.410	14.950	23.360	33.638
	0.8	0.813	3.251	7.315	13.005	20.320	29.261
	1	0.723	2.893	6.509	11.571	18.080	26.035
	2	0.459	1.836	4.130	7.342	11.472	16.520
	4	0.264	1.057	2.379	4.229	6.608	9.516

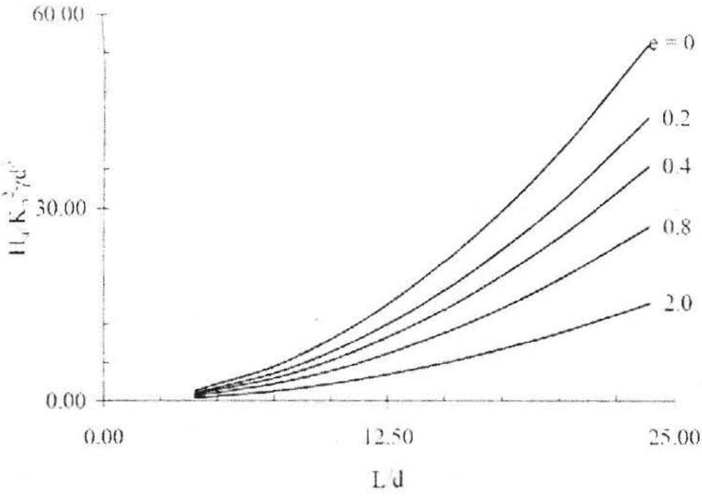

Fig. 15 Effect of eccentricity, for μ=100

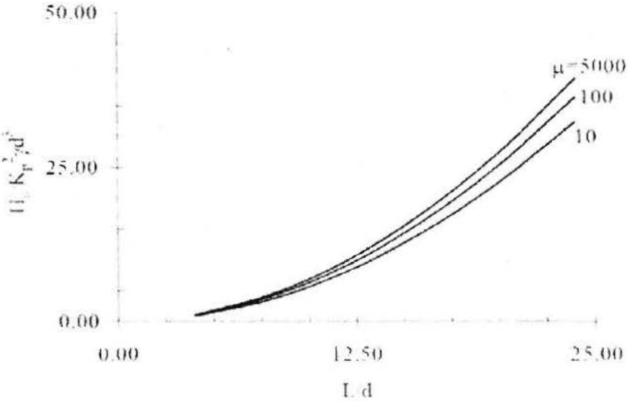

Fig. 16 L/d vs $H_u/K_p^2\gamma d^3$ for e = 0.4

References

Adams, J. I. and Radhakrishna, H. S. (1973): "The Lateral Capacity of Deep Augured Footings", *Proc. 8th Int. Conf. Soil Mech. Found. Engg.*, Moscow, Vol. 2, pp.1–8.

American Petroleum Institute (API) (1991): "Recommended Practice for Planning, Designing and Constructing Fixed Offshore Platforms", *API Recommended Practice 2A (RP2A)*, 19th edition, Washington, D.C.

Barton, Y. O. (1982): *Laterally Loaded Model Piles in Sand: Centrifuge Tests and Finite Element Analyses*, Ph. D. Thesis, University of Cambridge.

Briaud, J. L. and Smith, T. D. (1983): "Using the Pressuremeter Curve to Design Laterally Loaded Piles", *Proc, 15th Offshore Technology Conf.*, Houston, *Paper 4501*, pp. 495–502.

Broms, B. B. (1964): "Lateral Resistance of Piles in Cohesionless Soils", *Journal of the Soil Mechanics and Foundation Engineering Division,* ASCE, 90, pp.123-156.

Chari, T. R. and Meyerhof, G. G. (1983): "Ultimate Capacity of Rigid Piles under Inclined Loads in Sand", *Canadian Geotechnical Journal,* 20, pp. 849-854.

Fleming, W. G. K., Weltman, A. J., Randolph, M. F. and Elson, W. K. (1992): *Piling Engineering*, Surrey University Press, London.

Hansen, B. J. (1961): "The Ultimate Resistance of Rigid Piles against Transversal Forces", *Bulletin No. 12*, Danish Geotechnical Institute, Copenhagen, Denmark, pp. 5–9.

Kondner, R. L. and Zelasko, J. S. (1963): "A Hyperbolic Stress-Strain Formulation for Sands", *Proc. 2nd Pan Am. Conf. Soil Mech. Found. Engg.*, Brazil, 1, pp. 289-324.

Kulhawy, F. H. (1984): "Limiting Tip and Side Resistance: Fact or Fallacy", *Proc. Symp. on Design and Analysis of Pile Found.*, ASCE, New York, pp. 80–98.

Kulhawy, F. H. (1991): "Drilled Shaft Foundations", *Foundation Engineering Handbook.*, 2nd edition, Chapter 14, Fang, H.-Y. (Ed.), Van Nostrand Reinhold, New York.

Kulhawy, F. H., Trautmann, C. H., Beech, J. F., Rourke, T. D., MeGuire, W., Wood, W. A. and Capano, C. (1983): "Transmission Line Structure Foundations for Uplift-Compression Loading", *Rep. No. EL-2870,* Electric Power Research Institute, Palo Alto, California.

Meyerhof, G. G., Mathur, S. K., and Valsangkar, A. J. (1981): "Lateral Resistance and Deflection of Rigid Wall and Piles in Layered Soils", *Canadian Geotechnical Journal*, 18, pp. 159-170.

Meyerhof, G. G. and Sastry, V. V. R. N. (1985): "Bearing Capacity of Rigid Piles under Eccentric and Inclined Loads". *Canadian Geotechnical Journal*, 22, pp. 267-276.

Nabil, F. I. (1989): "Field Tests on Bored Piles Subject to Axial and Oblique Pull", *Journal of Geotechnical Engineering*, ASCE, 115, pp. 1588-1598.

NAVFAC (1982): "Foundations and Earth Structures", *Design Manual 7.2*, U.S. Department of the Navy, Alexandria.

Padmavathi, V., Saibaba Reddy, E. and Madhav, M. R. (2005): "Analysis of Laterally Loaded Rigid Piles in Sands Using Non-Linear Subgrade Reaction", *Indian Geotechnical Conference,* IGC - 2005, Ahmedabad, 2, pp. 27-30.

Patra, N. R. and Pise, P. J. (2001): "Ultimate Lateral Resistance of Pile Groups in Sand", *Journal of Geotechnical and Geoenvironmental Engineering*, ASCE, 127, pp. 481-487.

Poulos, H. G. and Davis, E. H. (1980): *Pile Foundation Analysis and Design*, John Wiley and Sons, New York.

Prakash, S. and Kumar, S. (1996): "Nonlinear Lateral Pile Deflection Prediction in Sands". *Journal of Geotechnical and Geoenvironmental Engineering*, ASCE, 122, pp. 130-138.

Prasad, Y. V. S. N. and Chari, T. R. (1999): "Lateral Capacity of Model Rigid Piles in Cohesionless Soils". *Soils and Foundations*, 39, pp. 21-29.

Randolph, M. F., Dolwin, J. and Beck, R. (1994): "Design of Driven Piles in Sand", *Geotechnique*, 44, pp. 427-448.

Matlock, H. and Reese, L. C. (1960): "Generalized Solutions for Laterally Loaded Piles", *Journal of the Soil Mechanics and Foundation Engineering Division*, ASCE, 86, pp. 63-91.

Reese, L. C., Cox, W. R. and Koop, W. D. (1974): "Analysis of Laterally Loaded Piles in Sand", *Proc. 6th Offshore Technology Conference*, Paper No. 2080, Houston, Texas, pp. 473-482.

Reese, L. C. and Matlock, H. (1956): "Non-Dimensional Solutions for Laterally Loaded Piles with Soil Modulus Assumed Proportional to Depth", *Proc. 8th Texas Conference on Soil Mechanics and Foundation Engineering,* Special Publication 29, Bureau of Engineering Research, University of Texas, Austin.

Shen, W. Y. and Teh, C. I. (2004): "Analysis of Laterally Loaded Piles in Soil with Stiffness Increasing with Depth". *Journal of Geotechnical and Geoenvironmental Engineering*, ASCE, 130, pp. 878-882.

Terzaghi, K. (1955): "Evaluation of Coefficients of Subgrade Reaction", *Geotechnique*, 5, pp. 297-326.

Tomlinson, M. J. (1986): *Foundation Design and Construction*, 5th edition, Pitman Books Ltd., London.

Wong, K. S. and Teh, C. I. (1995): "Negative Skin Friction on Piles in Layered Soil Deposits". *Journal of Geotechnical Engineering*, ASCE, 121, pp. 457-465.

Zhang, L., Silva, F. and Grismala, R. (2005): "Ultimate Lateral Resistance to Piles in Cohesionless Soils". *Journal of Geotechnical and Geoenvironmental Engineering*, ASCE, 131, pp. 78-83.